

perpolarizing potentials was related to the degree of depolarization produced by background excitatory synaptic bombardment or injury. Cells with 60 to 70 mv spikes exhibited minimum (3 to 5 mv) hyperpolarizations during paroxysmal EEG waves, whereas larger polarizing potentials (10 to 15 mv) were recorded in slightly depolarized cells with 40 to 50 mv spikes. Deteriorating cells depolarized to the level of spike inactivation exhibited augmented repolarizing potentials. In such neurons membrane repolarizations during the EEG spikes had a time-course similar to the hyperpolarizations observed prior to spike inactivation (Fig. 2, *E* or *F*). Changes in frequency and duration of surface EEG spikes or sharp waves were associated with parallel changes in repolarizing potentials (Fig. 2, *G* and *H*).

Our study establishes that EEG spikes or sharp waves are temporally related to synchronously developing membrane depolarizations and hyperpolarizations in neurons in epileptogenic foci. Depolarizations may or may not be associated with all-or-none discharges, whereas hyperpolarizations invariably produce inhibition of firing. The characteristics of these membrane potential changes are similar to those of prolonged postsynaptic potentials. This is particularly evident with respect to the hyperpolarizations or repolarizations which survive loss of the spike-generating mechanism and exhibit a relationship to membrane potential level expected for inhibitory postsynaptic potentials (7).

Although prolonged membrane potential changes and EEG discharges are closely related temporally, their relation with respect to polarity is variable as in the case of hippocampal seizure activities (3). The EEG spike or sharp wave in a lesion produced by freezing is a reflection of the sum of membrane depolarizations and hyperpolarizations in neurons located at various depths. Thus the polarity of the focal EEG discharge appears to be a consequence of variations in the magnitude and proportion of depolarizing, excitatory, and hyperpolarizing, inhibitory postsynaptic potentials generated in neurons in complex synaptic organizations (8, 9).

ELI S. GOLDENSOHN

DOMINICK P. PURPURA

Departments of Neurology and
Neurological Surgery, College of
Physicians and Surgeons,
Columbia University, New York 32

References and Notes

1. J. K. Merlis, in *Neuronal Physiopathology*, R. G. Grenell, Ed. (Harper and Rowe, New York, 1962); A. A. Ward, Jr., in *Intern. Rev. Neurobiol.* 3, 137 (1961).
2. C. L. Li, *J. Neurophysiol.* 22, 436 (1959).
3. E. R. Kandel and W. A. Spencer, *Exptl. Neurol.* 4, 162 (1961).
4. J. R. Atkinson, J. M. Macs, A. A. Ward, Jr., *Electroencephalog. Clin. Neurophysiol.* 13, 824 (1961).
5. T. G. Smith, Jr., and D. P. Purpura, *ibid.* 12, 59 (1960).
6. D. P. Purpura and B. Cohen, *J. Neurophysiol.* 25, 621 (1962).
7. J. C. Eccles, *Ergeb. Physiol. Biol. Chem. Exptl. Pharmacol.* 51, 299 (1961); H. Grundfest, in *Handbook of Physiology, Neurophysiology*, J. Field, Ed. (American Physiological Society, Washington, D.C., 1959), vol. 1, p. 147.
8. D. P. Purpura, *Intern. Rev. Neurobiol.* 1, 47 (1959).
9. Supported in part by the National Institute of Neurological Diseases and Blindness (B 1312-C5) and the United Cerebral Palsy Research and Education Foundation (R-135-62 C). One of us (E.S.G.) is a career research scientist, New York City Health Council; the other (D.P.P.) is a research career development fellow, National Institute of Neurological Diseases and Blindness.

24 December 1962

Xenon Difluoride and the Nature of the Xenon-Fluorine Bond

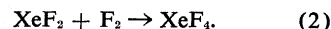
Abstract. Xenon reacts with fluorine to form XeF_2 which can be isolated before it reacts with fluorine to form XeF_4 . The linear configuration of XeF_2 with the 2.00-Å bond length and the vibrational force constants support the assignment of 10 electrons to the valence shell of xenon. Similar arguments support the assignment of 12 and 14 valence electrons respectively to xenon in XeF_4 and XeF_6 .

In their report on XeF_4 , Claassen, Selig, and Malm (1) noted a lower fluoride, which was identified by Chernick *et al.* (2) as XeF_2 . Smith's study (3) of the xenon-fluorine reaction resulted in a method of preparation of nearly pure XeF_2 . The molecular configuration, the Xe-F bond distance, and the vibrational force constants have been obtained from x-ray (4) and neutron (5) diffraction and from infrared and Raman spectra (6), and have led to some understanding of the nature of the Xe-F bond.

The loop used to study the Xe-F₂ reaction is shown in Fig. 1. The loop provides for examination of the infrared spectrum of the reaction mixture to determine composition or production rates. The circulating gas passes rapidly through the short hot zone where the reaction



occurs with a rate increasing as the partial pressure of Xe or F₂ is increased. XeF_4 is produced only when XeF_2 reacts with F₂,



The rate of Reaction 2 increases as the partial pressure of XeF_2 or F₂ is increased. Both reactions go faster as the temperature is increased. Reaction products were observed at temperatures as low as 270°C. Reaction 2 produces little XeF_4 if the reaction rates are kept low and if the XeF_2 is trapped out before it passes into the reaction zone. With care, nearly pure XeF_2 has been obtained. These conditions were satisfied by Weeks *et al.* (7) in their photochemical preparation of XeF_2 , while the reaction described by Claassen *et al.* (1) resulted in pure XeF_4 because the XeF_2 produced was retained in the closed reaction vessel with F₂ until it all reacted.

Xenon difluoride is remarkably similar to and difficult to separate from XeF_4 . It is a solid with a vapor pressure of 3.8 mm-Hg at 25°C and 318 mm-Hg at 100°C. It forms clear, brilliant crystals that grow to millimeter dimensions in a few hours. The solid melts at about 140°C and can be supercooled as much as 50°C without solidifying.

Two intense infrared bands in XeF_2 vapor have been observed at 555 cm⁻¹ and 213.2 cm⁻¹. The first, with no Q branch, has been assigned as ν_3 (asymmetric stretching) and the second, with a well defined Q branch, as ν_2 (bending). A third band observed at 1070 cm⁻¹ is the weak combination band $\nu_1 + \nu_3$, from which the infrared inactive vibration ν_1 may be obtained as 515 cm⁻¹. Band contours are characteristic of a linear symmetrical molecule. The P-R separation of ν_3 , 16 cm⁻¹, is inversely proportional to the square root of the moment of inertia and yields an estimate of 1.7 Å for the Xe-F distance, in accord with the more precise value obtained by diffraction. Raman lines for solid XeF_2 were found at 108 cm⁻¹ (intensity, 0.33), 497 cm⁻¹ (intensity, 1.00), 548 cm⁻¹ (intensity, 0.07), with an indication of another at 509 cm⁻¹. The first is probably a libration frequency; the second is clearly ν_{12} and the other two are ascribable to an impurity of XeF_4 . The fundamental frequencies for the vapor yield the following force constants (in millidynes per angstrom): k , (principal stretching constant), 2.85; k_{rr} (stretch-

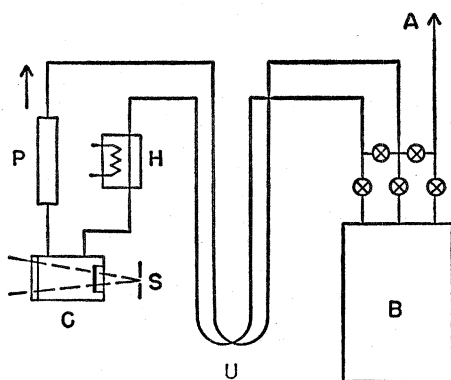


Fig. 1. Loop used to study Xe, F_2 , and XeF_2 reactions containing a piston pump P actuated by external magnets, a ballast volume B , U-tubes U , electrically heated zone H , and an infrared cell C , located in the beam of the spectrophotometer S . The loop is connected to a supply and evacuation manifold at A .

ing interaction constant), 0.11; and k_δ/l^2 (bending constant), 0.19.

A neutron diffraction study (5) shows that the crystal of XeF_2 consists of a body-centered tetragonal array of discrete parallel linear symmetric molecules, as illustrated in Fig. 2. The estimate of the Xe-F distance is 2.00 ± 0.01 Å, after correction for thermal displacements. The same structure has been obtained with less precision by x-ray diffraction (4).

The assignment of bonding electrons to the Xe $6s$ shell is ruled out by the short 2.00-Å Xe-F distance. There then

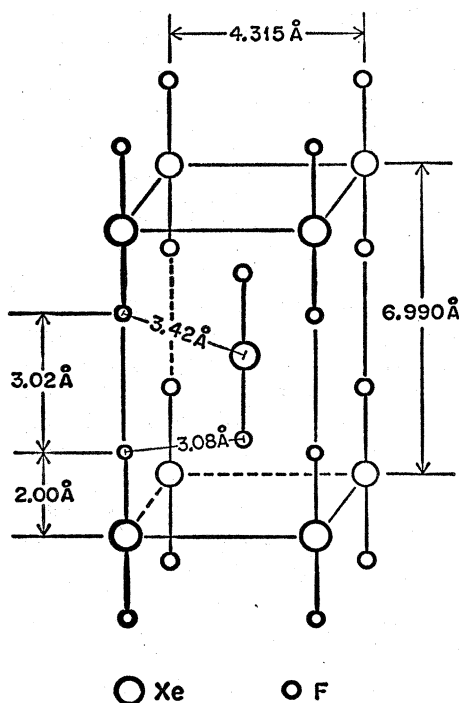


Fig. 2. Crystal structure of xenon difluoride as given by neutron diffraction.

remain three kinds of bonding which might be considered for XeF_2 : (A) The ionic model $F^-Xe^{++}F^-$, which involves six electrons in the xenon valence shell. (B) Two one-electron bonds which might be represented by resonance between F^-Xe^+-F and $F-Xe^+F^-$, with each bond having 50 percent covalent, 50 percent ionic character. This model has eight electrons in the Xe valence shell. (C) The covalent model $F-Xe-F$, which requires ten electrons in the Xe valence shell, with promotion to the $5d$ levels.

Each model can be linear. Thus, the observed configuration does not discriminate between them. Model A (the ionic model) would be expected to have a bond distance appreciably longer than 2.00 Å in view of the 2.345-Å bond length found for diatomic CsF (8) and 2.26 Å (estimated) for gaseous RbF . The pure ionic model can be ruled out on this basis. If the covalent radius for Xe is taken to be about 0.05 Å shorter than it is for iodine, the radius sum 1.95 Å should apply to the covalent model C. Model B, by analogy with ClF_3 and BrF_3 , should have a bond length 0.1 Å longer, about 2.05 Å. Thus a choice between models B and C cannot be made on the basis of bond length.

The bonding in ICl_2^- has been established to be of type B by Cornwell and Yamasaki's measurement of the nuclear quadrupole coupling of Cl (9). The vibration spectrum of ICl_2^- displays two remarkable characteristics resulting from this kind of bonding (10). The first is that the principal force constant, k_r , is small, about half the value for the ICl molecule. The second feature is that the interaction force constant, k_{rr} , is large, nearly a third of k_r , because stretching of one bond tends to make the resonance structure in which this bond is ionic more prominent, changing the nature of the bonding more than normally. This is in marked contrast to XeF_2 , in which $k_r=2.85$ mdy/Å (a high value) while $k_{rr}=0.11$ mdy/Å (a low value). The evidence thus favors model C with essentially covalent bonds and ten electrons in the xenon valence shell. In the hybridized sp^3d configuration, the collinear pd hybrid orbitals may be assigned for bonding and the three unshared pairs placed in sp^2 hybrid orbitals in the plane normal to the molecular axis.

For XeF_4 , knowledge of the planar square configuration (11) and the bond distance (12), 1.95 Å, supplemented

by the stretching force constant (13), also indicates covalent bonding, in this case with 12 electrons in the xenon valence shell and sp^3d^2 hybrid orbitals (14). The shorter distance in XeF_4 indicates more s -character to the bonding orbital than in XeF_2 .

The configuration of XeF_6 (15) has not yet been established. We presently favor a nonoctahedral structure since there is an infrared band at 1225cm^{-1} (16) which may be the first overtone of the XeF stretching vibration at 612cm^{-1} (15). A first overtone band is forbidden for a molecule with a center of symmetry. Covalent bonding with 14 electrons in the xenon valence shell and sp^3d^3 orbitals can lead to a nonoctahedral structure.

While bonding involving promoted d electrons has long been considered (17), there has been some question (18) whether any certain examples exist. The xenon fluorides appear to furnish these examples.

P. A. AGRON

G. M. BEGUN

HENRI A. LEVY

Chemistry Division, Oak Ridge National Laboratory, Oak Ridge, Tennessee

A. A. MASON

Physics Department,

University of Tennessee, Knoxville

C. G. JONES

D. F. SMITH

Technical Division, Oak Ridge Gaseous Diffusion Plant, Oak Ridge, Tennessee

References and Notes

- H. H. Claassen, H. Selig, J. G. Malm, *J. Am. Chem. Soc.* **84**, 3593 (1962).
- C. L. Chernick *et al.*, *Science* **138**, 136 (1962).
- D. F. Smith, *J. Chem. Phys.* **38**, 276 (1963).
- S. Siegel and E. Gebert, *J. Am. Chem. Soc.* **85**, 240 (1963).
- H. A. Levy and P. A. Agron, *ibid.* **85**, 241 (1963).
- G. M. Begun, A. A. Mason, D. F. Smith, vibration spectrum study in progress.
- J. L. Weeks, C. L. Chernick, M. S. Matheson, *J. Am. Chem. Soc.* **84**, 4612 (1962).
- A. Honig, M. Mandel, M. L. Stitch, C. H. Townes, *Phys. Rev.* **96**, 629 (1954).
- C. D. Cornwell and R. S. Yamasaki, *J. Chem. Phys.* **27**, 1060 (1957).
- W. B. Person *et al.*, *J. Chem. Phys.* **35**, 908 (1961).
- J. A. Ibers and W. C. Hamilton, *Science* **139**, 107 (1963); D. H. Templeton, A. Zalkin, J. D. Forester, S. M. Williamson, *J. Am. Chem. Soc.* **85**, 242 (1963).
- J. H. Burns, P. A. Agron, H. A. Levy, neutron diffraction study in progress.
- Take $\nu_1 = 543\text{cm}^{-1}$, $\nu_2 = 508\text{cm}^{-1}$, $\nu_3 = 586\text{cm}^{-1}$ for the frequencies given by Chernick *et al.* (2), and the XeF_4 stretching force constants differ only a little from the XeF_2 values. These are in marked contrast to ICl_4^- .
- Molecular orbital calculations (LCAO approximation) for XeF_2 and XeF_4 are reported by Lohr and Lipscomb (*J. Am. Chem. Soc.* **85**, 240 (1963)). The contribution of promoted Xe d orbitals is not considered. Within the set considered (Xe $d^5 sp^3$, F sp^3) the highest energy molecular orbitals were substantially Xe p ; thus the predicted structures appear to

be analogous to model A, but with strong polarization. The calculated energy minima, which appeared at 2.1 Å for XeF_2 and 2.4 Å for XeF_4 , are both somewhat larger than observed. In qualitative discussion, L. C. Allen [*J. Am. Chem. Soc.* **84**, 4344 (1962)] includes model C as a possibility, while K. S. Pitzer [*Science* **139**, 414 (1963)] and R. E. Rundle [*J. Am. Chem. Soc.* **85**, 112 (1963)] attribute the equivalent of type B bonding to the xenon fluorides. None of these authors have considered the implications of the vibration spectrum.

15. J. C. Malm, I. Sheft, C. L. Chernick, *J. Am. Chem. Soc.* **85**, 110 (1963); E. E. Weaver, B. Weinstock, C. P. Knop, *ibid.* **85**, 111 (1963).
16. D. F. Smith, infrared studies in progress.
17. See, for example, R. Gillespie and R. Nyholm, *Quart. Rev. London* **11**, 339 (1957).
18. E. E. Havinga and E. H. Wiebenga [*Rec. Trav. Chim.* **78**, 724 (1959)] discuss the situation for the polyhalide ions and interhalogen molecules.

8 February 1963

Antigens in Insulin Determinants of Specificity of Porcine Insulin in Man

Abstract. *Porcine insulin, which is distinguished from human insulin only in the amino acid at the C terminal of the B chain, is antigenic in man. Even if the last amino acid or the last eight amino acids are removed from the C terminus of the B chain of insulin, the altered insulin still reacts with human antibodies to porcine insulin; thus, the antigenic determinant of porcine insulin is located in a part of the molecule where the amino acid sequence is the same as it is in the corresponding part of the human insulin molecule.*

As a result of experiments with insulin labeled with I^{131} , insulin-binding antibodies have been demonstrated in the serums of virtually all human subjects treated with commercial mixtures of bovine and porcine insulin (1, 2). Insulin-binding antibody is never observed in subjects who have never been treated with insulin. Although insulin antibodies react with insulins derived from a large variety of mammalian (3, 4) and piscine (5) species, the reaction is almost always strongest with bovine insulin (3). Porcine insulin (6) differs from human insulin (7) only in containing alanine instead of threonine as the C terminal amino acid of the B chain (B 30) whereas bovine insulin (6) shows additional differences in residues 8 and 10 of the A chain. Differences in immunologic reactivities of insulins from four different ungulate species (3) could be related to differences in the 8 to 10 region of the A chain (6) suggesting that this region

of bovine insulin might constitute a site of antigenicity in man (3).

In the present study human subjects were immunized with pure porcine insulin in order to determine whether the C terminus of the B chain (B 30) is a site of antigenicity in man. Five newly discovered diabetic persons were treated with NPH (neutral protamine Hagedorn) porcine insulin at doses of 10 to 40 units per day. Insulin-binding antibodies were detectable in all subjects within 6 weeks to 3 months after institution of therapy. In three cases, antibody concentrations were sufficient to conduct these studies. Similar results were obtained in all subjects.

I^{131} -labeled insulin was prepared from crystalline bovine or porcine insulin or from desoctapeptide bovine insulin (insulin lacking the last eight amino acids of the C terminus of the B chain) according to methods described previously (8) or according to the method of Hunter and Greenwood (9). Mixtures of insulin and antiserum were prepared so that the concentrations of I^{131} -labeled insulin were always the same even though the concentrations of unlabeled intact insulin or insulin derivative from different species varied. After incubation for 2 to 3 days at 4°C, aliquots of the mixtures were applied to strips of Whatman 3-MM filter paper (10) which were used for electrophoretic or chromatoelectrophoretic separation of insulin- I^{131} bound to antibody, and "free" (unbound) insulin- I^{131} (1). Free insulin- I^{131} is adsorbed firmly to this paper at the site of application whereas insulin- I^{131} bound by antibody migrates with the serum proteins (1) in the region between β - and γ -globulin (11). The following insulin preparations were used: crystalline porcine insulin, desalanine porcine insulin (insulin lacking B 30), crystalline bovine insulin, desoctapeptide bovine insulin and crystalline human insulin (12). The ratio between insulin- I^{131} bound to antibody and free insulin- I^{131} is plotted as a function of the concentration of unlabeled insulin or insulin derivative in the mixture (Figs. 1-3). Insulin-binding antibodies in the serums of subjects immunized with porcine insulin reacted almost as well with desalanine porcine insulin, desoctapeptide bovine insulin, and human insulin as with the intact porcine and bovine insulins when competing against the binding of porcine insulin- I^{131} or bovine insulin- I^{131} (Figs. 1 and 2). The reac-

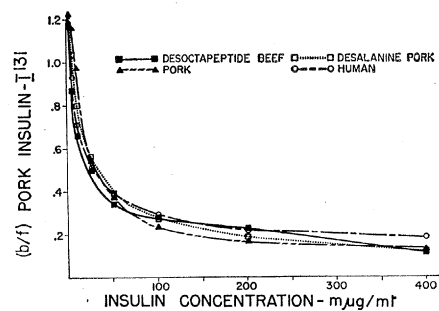


Fig. 1. Antibodies to porcine insulin. Plasma dilution 2:5. The ratio, b/f, of antibody bound (b) to free (f) bovine or porcine insulin labeled with I^{131} as a function of concentration of the unlabeled insulins in serum from a human subject treated with pure porcine NPH insulin for 7 months.

tion with porcine insulin- I^{131} was slightly stronger than with bovine insulin- I^{131} . These results are in contrast to observations with antisera from subjects treated with commercial mixtures of bovine and porcine insulin, in which human insulin (3, 13) and desoctapeptide bovine insulin (2) generally compete much less effectively than intact bovine insulin against the binding of bovine insulin- I^{131} . Binding of desoctapeptide insulin- I^{131} in antisera to porcine insulin was also demonstrated directly by paper electrophoresis.

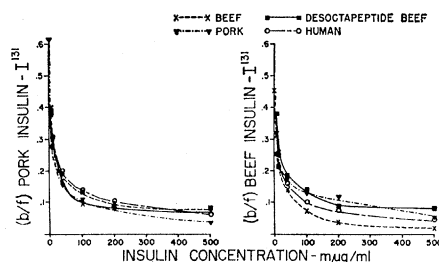


Fig. 2. Antibodies to porcine insulin. Plasma dilution, 1:5. Same patient as shown in Fig. 1 after 11 months of therapy with pure porcine NPH insulin.

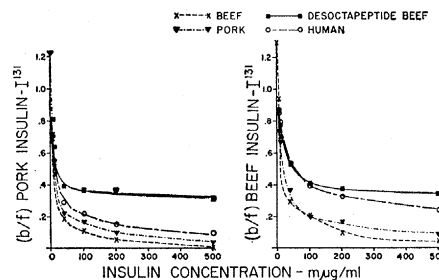


Fig. 3. Antibodies to bovine and porcine insulin in serum of same patient after 5½ months of further therapy with bovine NPH insulin. Plasma dilution 1:5.